

Gravity-dependent stick-slip dynamics in penetration experiments on simulated regolith

JACK FEATHERSTONE ¹, ROBERT BULLARD,¹ TRISTAN EMM,¹ ANNA JACKSON,¹ RILEY REID,¹ SEAN SHEFFERMAN,²
ADRIENNE DOVE ², JOSHUA COLWELL ², JONATHAN E. KOLLMER ^{1,3} AND KAREN E. DANIELS ¹

¹*Department of Physics, North Carolina State University, Raleigh, NC, 27675, USA*

²*Florida Space Institute and Department of Physics, University of Central Florida, Orlando, FL, 32816, USA*

³*Universität Duisburg-Essen, Lotharstr. 1, 47057 Duisburg, Germany*

(Received December 22, 2024; Revised; Accepted)

Submitted to The Planetary Science Journal

ABSTRACT

The surfaces of many planetary bodies, including asteroids and small moons, are covered with dust to pebble-sized regolith held weakly to the surface by gravity and contact forces. Understanding the reaction of regolith to an external perturbation will allow for instruments including sensors and anchoring mechanisms for use on such surfaces to implement optimized design principles. We analyze the behavior of a flexible probe inserted into loose regolith simulant as a function of probe speed and ambient gravitational acceleration to explore the relevant dynamics. The EMPANADA experiment (Ejecta-Minimizing Protocols for Applications Needing Anchoring or Digging on Asteroids) flew on several parabolic flights. It employs a classic granular physics technique, photoelasticity, to quantify the dynamics of a flexible probe during its insertion into a system of bi-disperse, cm-sized model grains. We identify the grain-scale forces throughout the system for probe insertion at a variety of speeds and for four different levels of gravity: terrestrial, martian, lunar, and microgravity. We identify discrete, stick-slip failure events that increase in both magnitude and frequency as a function of the gravitational acceleration. In microgravity environments, stick-slip behaviors are negligible, and we identify that faster probe insertion can suppress stick-slip behaviors where they are present. We conclude that the mechanical response of regolith on rubble pile asteroids is likely quite distinct from that found on larger planetary objects. Techniques borrowed from Earth-based granular physics experiments provide a promising set of methods for future work analyzing both local and global particle rearrangement events in microgravity conditions.

1. INTRODUCTION

Understanding how regolith rearranges when disturbed is integral to developing safe and efficient techniques for sample collection and anchoring on small planetary bodies. The surfaces of asteroids, moons, and even certain planets are characteristically described as a weakly interacting collection of heterogeneous grains. Such bodies could include our moon (Nash et al. 1993), as well as numerous near-Earth asteroids (Hestroffer et al. 2019). Specific examples of the latter include (101955) Bennu (Barnouin et al. 2019) and (162173) Ryugu (Watanabe et al. 2019), which have indeed been shown, through the OSIRIS-REx and Hayabusa2 mis-

sions respectively, to be composed of loosely bound rubble. Many questions regarding the formation (Cheng et al. 2020; Michel et al. 2020), surface features (Shinbrot et al. 2017; Bogdan et al. 2020), and mechanical stability (Sánchez & Scheeres 2020; Scheeres et al. 2010) of these asteroids still remain open.

There have been a number of numerical simulations (Maurel et al. 2018; Thuillet et al. 2018) as well as laboratory experiments (Colwell & Taylor 1999; Colwell et al. 2008; Altshuler et al. 2014; Li et al. 2016; Brisset et al. 2018; Brisset, J. et al. 2020) on low-velocity impacts onto simulated regolith surfaces under low gravity conditions. These impacts are not only relevant for understanding the formation of these bodies, but can also give insight into the inner composition of an asteroid (Quillen et al. 2019). For more detailed exploration, however, sampling the surface is necessary.

The recent sample collection by NASA’s OSIRIS-REx mission is an example of how instrumentation methods depend on the details of granular-structure interactions. The Touch-And-Go Sample Acquisition Mechanism (TAGSAM) involved expelling pressurized nitrogen gas to dislodge regolith from the surface (NASA 2020a), which was then captured within the sampling head (NASA 2020b). Two complications ensued during successful completion of the sample collection: it was not immediately clear how far the probe penetrated into the regolith surface, and an over-collection of regolith occurred (NASA 2020c). Hayabusa2’s instruments take a similar approach to those of the OSIRIS-REx mission, capturing ejected regolith after disturbing the surface (Sawada et al. 2017). In this case, the disturbance is caused by a projectile, but the underlying dynamics still depend sensitively on the details of the granular material. A better understanding of the material properties (e.g. effective stiffness) of granular materials under low gravity conditions would aid in the design of future regolith collection missions.

In terms of mechanically manipulating and collecting a sample, there are presently no established safe and effective protocols to guide the interaction of space probes with low-gravity, poorly-consolidated material (Wilkinson et al. 2005). For rubble-pile asteroids, where the escape velocities can be on the order of cm/s (Sánchez & Scheeres 2014; Daniels 2013), the development of ejecta-minimizing operations will be particularly important. One promising technique, inspired by the growth of plant roots (Kolb et al. 2012; Wendell et al. 2012), is the use of slow, flexible probes (Kollmer et al. 2016). The dynamics of such a flexible, slender probe interacting with a granular material in low gravity are yet unexplored.

The Artemis program, which outlines a plan for the progressive development of a human presence on the moon over the next decade, presents another important context for better-understanding the interactions of probes and diggers with surface regolith. Because NASA and other international partners plan to establish semi-permanent structures (NASA 2019; Woerner et al. 2016), these would require both constructing stable foundations on a surface composed of coarse regolith (Wilkinson et al. 2005), and material handling for in-situ resource utilization (Zacny et al. 2018).

In this paper, we present investigations of a prototypical surface interaction: the insertion of a flexible probe into a granular medium under various levels of gravity. This project is named EMPANADA (Ejecta-Minimizing Protocols for Applications Needing Anchoring or Digging on Asteroids), and is inspired by previous work on

the PRIME project (Brisset et al. 2018). In these new experiments, we slowly insert a flexible intruder into a vertical bed of round, quasi-two-dimensional elastic grains. Sample images from this setup in three different levels of gravity – martian, lunar, and micro – are shown in Figs. 1a, 1b, and 1c. These three gravitational accelerations were achieved during a parabolic flight campaign, while terrestrial gravity experiments were performed after the same apparatus was returned to the lab. By varying the insertion speed of the probe for each level of gravity, we are able to identify how these parameters impact the overall dynamics of the granular bed.

Our analysis primarily considers videos of the particle dynamics taken as the probe is driven into the surface of the granular material, using the apparatus shown in Fig. 1d. The model regolith comprises grains made of a photoelastic material, a technique for experimentally investigating internal forces within granular systems (Daniels et al. 2017; Abed Zadeh et al. 2019). We show that bulk descriptors, such as the brightness of each video frame, are able to encode the main features of the local grain dynamics with sufficient precision to identify when slip events take place. Therefore, the time series of these estimated forces is taken as a proxy for the dynamics of the grains during the insertion process.

We find that both the magnitude and frequency of rearrangements increase as a function of the gravitational acceleration. For experiments at terrestrial, martian, and lunar gravity, faster insertion speeds suppress dynamics within the granular bed. Specifically, the number of discrete stick-slip failure events is reduced, without a significant increase in the intensity of each individual event; this is surprising because a faster probe injects more kinetic energy. For the microgravity case, we are not able to identify any specific relationship between insertion speed and granular dynamics; in this regime, the behavior of the grains is not well described by discrete stick-slip events (Albert et al. 2001).

2. METHODS

We performed experiments on the apparatus shown in Fig. 1d, which was both flown on parabolic flights and used in laboratory experiments on earth’s surface. The setup centers around a backlit, vertical bed of photoelastic disks about 1 cm in diameter, and a flexible probe mounted on a motor driven slider. There are controls for the motor and LEDs on the front, as well as a mount point for a camera such that it captures videos of the probe insertion dynamics. The probe mount also includes a load cell, which measures the net force acting on the probe as it descends into the grains. We conducted

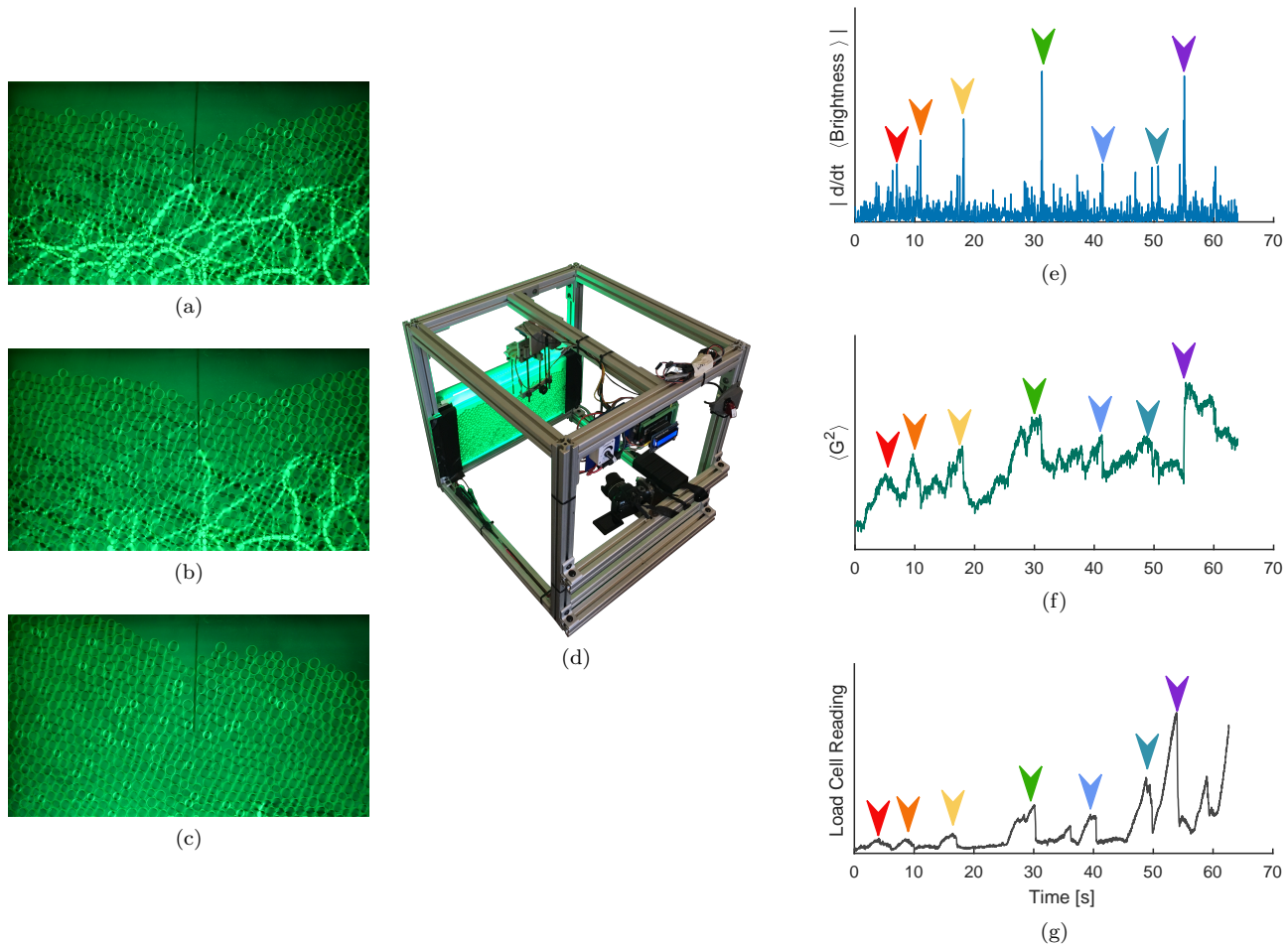


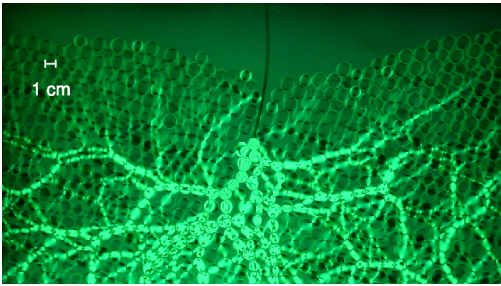
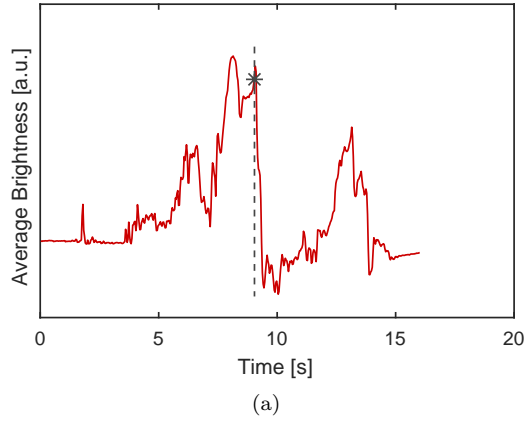
Figure 1. Qualitative comparison of video collected from (a) martian, (b) lunar, and (c) microgravity trials. The martian and lunar trials show more prominent inter-particle force chains as compared to the microgravity trial. (d) The EMPANADA-2D apparatus used to collect data, showing the backlit photoelastic particles, camera, and motor assembly. Comparison between the granular dynamics as measured by (e) the time derivative of the average image brightness, (f) the average G^2 (local gradient, squared) of the image brightness, and (g) the load cell readings on the probe. Arrow colors indicate the same event across all three graphs.

experiments – consisting of the probe being driven into the granular material – under four different gravity conditions: terrestrial, martian, lunar, and microgravity. The latter three experiments were conducted during a parabolic flight campaign (Zero-G Corporation); terrestrial trials were completed on the same apparatus after its return.

The photoelastic particles, having stress-dependent polarization, indicate the strength of local, inter-particle forces via their brightness (Daniels et al. 2017; Abed Zadeh et al. 2019). Video of the granular bed allows for observation of the brightness in each frame throughout the insertion process, giving a profile of the net forces in the system. This metric can then be modified and extended to highlight the general behavior of the insertion process, including identifying discrete stick-slip events. Due to safety considerations, the parti-

cle enclosure is constructed from acrylic sheets; these act as fractional waveplates, and slightly rotate the polarization of the light transmitted through the particles. This effect manifests as some force chains appearing dark in the video frames; we adjusted for this by preprocessing the images to highlight the force chains, regardless of their orientation in the raw images. This process also filtered out the majority of the particle outlines, further reducing the amount of noise in the analyzed data. A comparison between analyzing the edited images versus the raw images has shown that both provide the same overall trends, with the former exhibiting less noise.

During each trial, the granular bed was probed by a flexible intruder made from acrylic and about 10 cm long, with cross-sectional area ranging from 2-4 mm². The probe is flexible enough to navigate through the grains by either bending itself or slipping past individ-

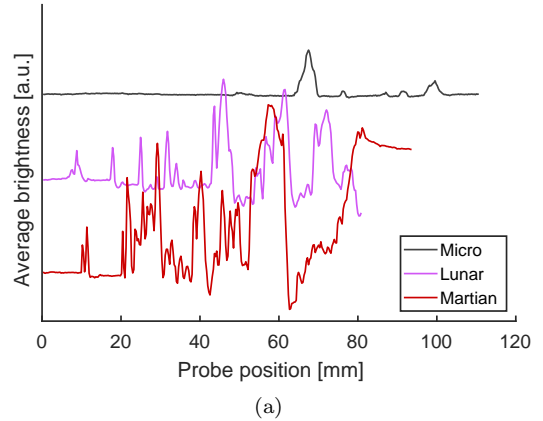


(b)

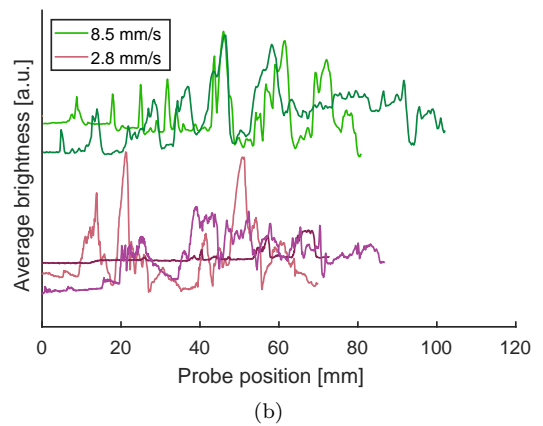
Figure 2. (a) The plot of average frame brightness for a martian trial. Annotation on the plot represents the time that corresponds to the frame shown in (b). The grains are made of photoelastic materials, meaning the regions under higher stress appear brighter.

ual particles, both of which can cause varying levels of disturbance in the system. The probe is attached to the stepper motor via a load cell, which is driven into the medium at a constant speed. This load cell records forces parallel to the probe as it traverses the system.

Although the load cell is able to directly record the forces on the probe, we primarily utilize the video recordings of the insertion throughout the analysis presented here. Besides the load cell readings not being available for every trial, we find that there are some events that are not local enough to the probe to be recorded in the direct force measurements. From the video data, it is possible to identify both events that are directly in contact with the probe, as well as rearrangements that propagate elsewhere in the medium. A comparison between the direct measurement and this image analysis (Figs. 1e, 1f, 1g) demonstrates that simply measuring the brightness encapsulates the information present from the probe, along with additional information. While granular physics experiments often use the local gradient of image brightness (the G^2 method, [Abed Zadeh et al. \(2019\)](#)) to quantify forces instead of the average brightness, we found that the brightness was



(a)



(b)

Figure 3. (a) The average brightness of each video frame for a trial in each level of gravity simulated during the parabolic flight campaign, all with probe insertion speed of 8.5 mm/s. (b) The brightness profiles for several trials conducted in lunar gravity, with multiple trials at the same insertion speed grouped together.

better-suited to counting the number of discrete events and have therefore used that measure in our analyses.

To gather data in lower gravity conditions, the apparatus was flown on a parabolic flight campaign (Zero-G Corporation), yielding 41 total trials, each corresponding to martian (6), lunar (5), or microgravity (30). The probe insertion process was run at several different speeds for each level of gravity over the course of two flights. Although some g -jitter was present during these flights, the majority of the trials were suitable for semi-quantitative analysis. Those which we identified to have major deviations from the expected conditions – e.g. net acceleration pointing upwards during certain microgravity trials – were excluded from our analysis. After the flight campaign, the apparatus was brought back to the lab, and additional data was taken in terrestrial gravity. These trials were able to cover a more extensive range of speeds. The final data set includes trials run at three

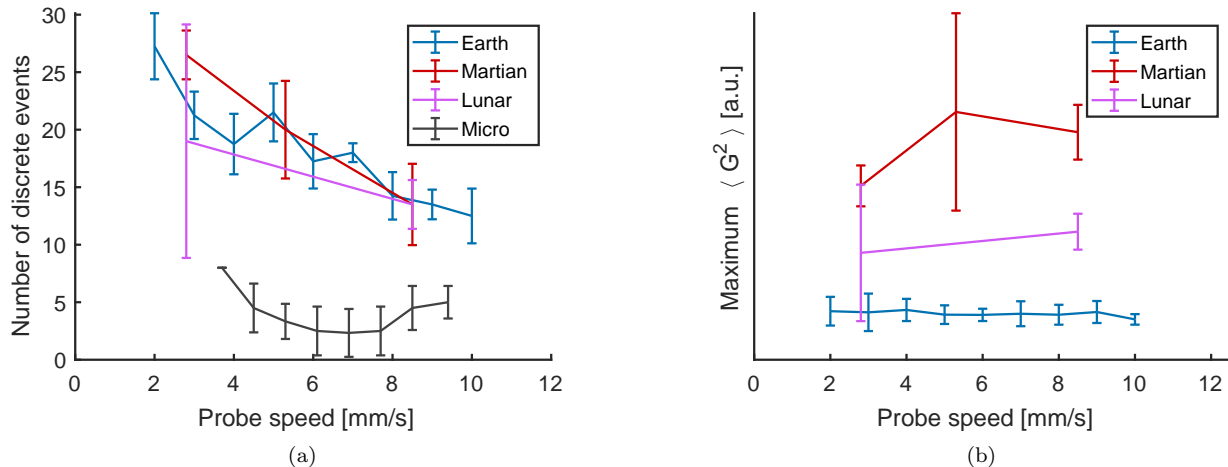


Figure 4. (a) The discrete number of slipping events for each trial, counted as local maxima in the discretized time derivative of the average frame brightness. Appropriate statistical error bars are included for gravity/speed pairs that had more than one data point. (b) A comparison of the maximum local gradient squared during the terrestrial, martian, and lunar trials, taken as a proxy for the maximum instantaneous force. Each connected set of points (same gravity) were taken under the same lighting conditions, but cannot be compared between sets.

”planetary” gravities – lunar, martian, and earth – as well as asteroid-like microgravity.

A sample frame from a trial can be seen in Fig. 2b, with the corresponding brightness plot shown above (Fig. 2a), where the image time is indicated by the dashed line. The force chains can be identified as bright paths through the grains. As can be seen in the video frame, the probe is currently exerting a force on a single grain, which then propagates through the rest of the system. Once the force becomes strong enough, the probe will slip off the grain it is in contact with, causing nearby grains to reconfigure. This can be identified in the brightness plot, represented as the sharp decline immediately after the current time marked on the figure.

Motivated by this behavior, we next look at the time derivative of the brightness as a metric for how the medium is changing throughout the insertion process. This is done using a central difference stencil on the average frame brightness. To complement this method, a comparison is made with the load cell readings on the probe, which recorded data for a limited set of the runs. This comparison (Figs. 1e, 1f, 1g) demonstrates that the global image brightness provides similar information about the physical dynamics of the system as the local force readings. In the following analysis, we therefore choose to primarily use the global image brightness, as it is available for all of our experimental runs.

3. RESULTS

Figure 3a shows a comparison of the average brightness (representing the total interparticle forces in the system) during probe insertion for 3 different trials, cov-

ering the three extraterrestrial levels of gravity that were tested – martian, lunar, and microgravity. Qualitatively, higher gravitational acceleration gives a more sharply peaked average brightness, corresponding to stronger forces throughout the granular bed. Martian and lunar gravity show easily identifiable stick-slip events in the form of local maxima in the time dependent intensity data, confirmed by visual inspection of the corresponding videos. The insertion dynamics in microgravity exhibits more subtle behavior. There are features of the brightness curve that can be described as discrete events, but they don’t represent the dominant pathway for spatial reconfiguration. Per this behavior, we can show (see Fig. 4a) that attempting to describe a microgravity system as a sequence of stick-slip events – as would be done for the other trials – would not be appropriate.

Unlike the comparison between different levels of gravity, different insertion speeds don’t present an immediately recognizable trend in the corresponding granular dynamics. This can be seen in Fig. 3b, where a comparison of different speeds is shown for five lunar gravity trials. On average, the trials at lower speeds display no obvious differences from the ones conducted at higher speeds; a more quantitative analysis including additional trials would be required to identify any trends. This is representative of the other three levels of gravity, as similar comparisons for these cases also showed no significant qualitative differences.

To provide a more quantitative analysis, we define a *slipping event* as a local maxima in the discretized time derivative of the brightness of each experimental run, provided that it is sufficiently chronologically displaced

from other maxima by a cutoff time $t_c = 0.5$ s. Figure 4a visualizes this metric evaluated for all of the levels of gravity and all insertion speeds. For the planetary levels of gravity (all but microgravity), there is a clear downward trend in the number of discrete slipping events for higher speeds, which is reasonably within the statistically-calculated error bars. This demonstrates that for the insertion protocol used here (constant driving velocity), a higher insertion speed suppresses stick-slip behavior in conditions with significant gravity. For the microgravity case, there is not a strong trend to be seen, confirming our qualitative predictions that discrete rearrangements do not properly characterize the granular dynamics in this case; instead, the behavior is more fluid-like.

We next turn our attention to the intensity associated with each of these events. We evaluated the maximum frame-averaged G^2 value for each video – representing the maximum magnitude of instantaneous force – which is shown in Fig. 4b. Microgravity has been excluded from this comparison since it is not well-described by discrete events. No significant increase or decrease can be seen for any of the trials when considering the statistically-determined error bars. This demonstrates that the frequency of events is more strongly a function of the insertion speed than the intensity, although more data would be needed to establish this quantitatively.

4. CONCLUSIONS

Considering the frequency of stick-slip events (Fig. 4a) and their intensities (Fig. 4b) together suggests that the decrease in frequency at higher speeds is the sole effect of varying the insertion speed. We therefore conclude that the overall disturbance in the granular medium is minimized at higher speeds for situations in which significant gravity is present. For these cases, the acceleration due to gravity is strong enough that looking at discrete failure events captures a significant portion of the granular dynamics.

Taking a broader perspective, the disturbance minimization by higher insertion velocity must be limited by two constraints. First, the flexibility of the probe at some point will transition from plowing through the material to bending (Algarra et al. 2018). The other limit is the inertia of the particles. For interactions faster than the speed of sound in the material, one would expect to produce a shock (Hancock et al. 2020). This is especially relevant considering that the speed of sound in a granular material is a function of confining pressure and therefore ambient gravity (Gómez et al. 2012).

We therefore propose that an optimum insertion velocity must exist, for which disturbances of the granular bed are minimized, and that further experiments are needed to map out these dependencies.

For the microgravity trials, a dependence on insertion velocity was not observed, as exemplified by the rather flat curve in Fig. 4a. This is also qualitatively supported by the lack of extended force chains present in the microgravity images (Fig. 1c). In this regime, a different metric would need to be identified for evaluating the granular dynamics. Candidates for this as-of-yet unknown metric could include a quantification of creep or fragile states selection by the intruder, or an analysis of the state of rigidity the granular system as in Liu et al. (2020). The dynamics of inserting a flexible intruder into a granular medium is also a current topic of interest within the granular physics community (Algarra et al. 2018; Mojdehi et al. 2016), from which additional methods can be drawn. While there are similarities between the terrestrial and microgravity cases, experimental investigations in terrestrial gravity cannot reasonably be scaled to describe the microgravity case. The singular nature of the microgravity case necessitates in-situ experiments to properly quantify the dynamics.

In summary, we have shown that techniques borrowed from earth-based granular physics are adaptable to describe regolith dynamics on planetary bodies. For most of the situations we consider, a single metric is able to describe the majority of the granular dynamics. For the case in which this single, discrete measure is not applicable, we expect that other methods from granular physics will properly describe the more subtle behavior. Importantly, methods from the granular materials community allow for direct investigations of the interparticle forces throughout a granular system in a variable gravity environment to characterize both local and global phenomena of regolith in astrophysical contexts.

ACKNOWLEDGMENTS

This work was funded by NASA Grant number 80NSSC18K0269 (REDDI), along with with undergraduate student funding from both the NC State Office of Undergraduate Research and the NC State Provost’s Professional Experience Program. JK acknowledges funding by the German Aerospace Center DLR with funds provided by the Federal Ministry for Economic Affairs and Energy (BMWi) via Grant Number 50WM1943.

REFERENCES

- Abed Zadeh, A., Bares, J., Brzinski, T. A., et al. 2019, *Granular Matter*, 21, 83, doi: [10.1007/s10035-019-0942-2](https://doi.org/10.1007/s10035-019-0942-2)
- Albert, I., Tegzes, P., Albert, R., et al. 2001, *Physical Review E*, 64, 031307, doi: [10.1103/PhysRevE.64.031307](https://doi.org/10.1103/PhysRevE.64.031307)
- Algarra, N., Karagiannopoulos, P. G., Lazarus, A., Vandembroucq, D., & Kolb, E. 2018, *Physical Review E*, 97, 022901, doi: [10.1103/PhysRevE.97.022901](https://doi.org/10.1103/PhysRevE.97.022901)
- Altshuler, E., Torres, H., González-Pita, A., et al. 2014, *Geophysical Research Letters*, 41, 3032, doi: <https://doi.org/10.1002/2014GL059229>
- Barnouin, O. S., Daly, M. G., Palmer, E. E., et al. 2019, *Nature Geoscience*, 12, 247, doi: [10.1038/s41561-019-0330-x](https://doi.org/10.1038/s41561-019-0330-x)
- Bogdan, T., Kollmer, J. E., Teiser, J., Kruss, M., & Wurm, G. 2020, *Icarus*, 341, 113646, doi: <https://doi.org/10.1016/j.icarus.2020.113646>
- Brisset, J., Colwell, J., Dove, A., et al. 2018, *Progress in Earth and Planetary Science*, 5, 73, doi: [10.1186/s40645-018-0222-5](https://doi.org/10.1186/s40645-018-0222-5)
- Brisset, J., Cox, C., Anderson, S., et al. 2020, *A&A*, 642, A198, doi: [10.1051/0004-6361/202038665](https://doi.org/10.1051/0004-6361/202038665)
- Cheng, B., Yu, Y., Asphaug, E., et al. 2020, *Nature Astronomy*, Oct (published online), doi: [10.1038/s41550-020-01226-7](https://doi.org/10.1038/s41550-020-01226-7)
- Colwell, J. E., & Taylor, M. 1999, *Icarus*, 138, 241, doi: [10.1006/icar.1998.6073](https://doi.org/10.1006/icar.1998.6073)
- Colwell, J. E., Sture, S., Cintala, M., et al. 2008, *Icarus*, 195, 908, doi: [10.1016/j.icarus.2007.12.019](https://doi.org/10.1016/j.icarus.2007.12.019)
- Daniels, K. E. 2013, in *Asteroids: Prospective Energy and Material Resources*, ed. V. Badescu (Berlin, Heidelberg: Springer), 271–286, doi: [10.1007/978-3-642-39244-3_11](https://doi.org/10.1007/978-3-642-39244-3_11)
- Daniels, K. E., Kollmer, J. E., & Puckett, J. G. 2017, *Review of Scientific Instruments*, 88, 051808, doi: [10.1063/1.4983049](https://doi.org/10.1063/1.4983049)
- Gómez, L. R., Turner, A. M., & Vitelli, V. 2012, *Physical Review E*, 86, 041302, doi: [10.1103/PhysRevE.86.041302](https://doi.org/10.1103/PhysRevE.86.041302)
- Hancock, K., DeMartini, J. V., Richardson, D. C., & Tancredi, G. 2020, *Bulletin of the AAS*, 52, <https://baas.aas.org/pub/2020n6i104p03/release/1>
- Hestroffer, D., Sánchez, P., Staron, L., et al. 2019, *The Astronomy and Astrophysics Review*, 27, 6, doi: [10.1007/s00159-019-0117-5](https://doi.org/10.1007/s00159-019-0117-5)
- Kolb, E., Hartmann, C., & Genet, P. 2012, *Plant and Soil*, 360, 19, doi: [10.1007/s11104-012-1316-2](https://doi.org/10.1007/s11104-012-1316-2)
- Kollmer, J. E., Lindauer, S., & Daniels, K. E. 2016, in *ASCE Earth and Space 2016 Conference*, Orlando, FL
- Li, Y., Dove, A., Curtis, J. S., & Colwell, J. E. 2016, *Powder Technology*, 288, 303, doi: [10.1016/j.powtec.2015.11.022](https://doi.org/10.1016/j.powtec.2015.11.022)
- Liu, K., Kollmer, J. E., Daniels, K. E., Schwarz, J. M., & Henkes, S. 2020, *Physical Review Letters* (in press), arXiv:2006.00557. <http://arxiv.org/abs/2006.00557>
- Maurel, C., Michel, P., Biele, J., Ballouz, R.-L., & Thuillet, F. 2018, *Advances in Space Research*, 62, 2099, doi: [10.1016/j.asr.2017.05.029](https://doi.org/10.1016/j.asr.2017.05.029)
- Michel, P., Ballouz, R.-L., Barnouin, O. S., et al. 2020, *Nature Communications*, 11, 2655, doi: [10.1038/s41467-020-16433-z](https://doi.org/10.1038/s41467-020-16433-z)
- Mojdehi, A. R., Tavakol, B., Royston, W., Dillard, D. A., & Holmes, D. P. 2016, *Extreme Mechanics Letters*, 9, Part 1, 237, doi: [10.1016/j.eml.2016.03.022](https://doi.org/10.1016/j.eml.2016.03.022)
- NASA. 2019, *Artemis Moon Program Advances – The Story So Far*. <http://www.nasa.gov/artemis-moon-program-advances>
- . 2020a, *OSIRIS-REx*. <http://www.nasa.gov/osiris-rex>
- . 2020b, *NASA’s OSIRIS-REx Spacecraft Collects Significant Amount of Asteroid*. <https://www.nasa.gov/press-release/nasa-s-osiris-rex-spacecraft-collects-significant-amount-of-asteroid>
- . 2020c, *Second Rehearsal Puts OSIRIS-REx on a Path to Sample Collection*. <http://www.nasa.gov/feature/goddard/2020/second-rehearsal-puts-osiris-rex-on-path-to-sample-collection>
- Nash, D. B., Salisbury, J. W., Conel, J. E., Lucey, P. G., & Christensen, P. R. 1993, *Journal of Geophysical Research: Planets*, 98, 23535, doi: [10.1029/93JE02604](https://doi.org/10.1029/93JE02604)
- Quillen, A. C., Zhao, Y., Chen, Y., et al. 2019, *Icarus*, 319, 312, doi: [10.1016/j.icarus.2018.09.032](https://doi.org/10.1016/j.icarus.2018.09.032)
- Sawada, H., Okazaki, R., Tachibana, S., et al. 2017, *Space Science Reviews*, 208, 81, doi: [10.1007/s11214-017-0338-8](https://doi.org/10.1007/s11214-017-0338-8)
- Scheeres, D. J., Hartzell, C. M., Sánchez, P., & Swift, M. 2010, *Icarus*, 210, 968, doi: [10.1016/j.icarus.2010.07.009](https://doi.org/10.1016/j.icarus.2010.07.009)
- Shinbrot, T., Sabuwala, T., Siu, T., Vivar Lazo, M., & Chakraborty, P. 2017, *Physical Review Letters*, 118, 111101, doi: [10.1103/PhysRevLett.118.111101](https://doi.org/10.1103/PhysRevLett.118.111101)
- Sánchez, P., & Scheeres, D. J. 2014, *Meteoritics & Planetary Science*, 49, 788, doi: <https://doi.org/10.1111/maps.12293>
- . 2020, *Icarus*, 338, 113443, doi: [10.1016/j.icarus.2019.113443](https://doi.org/10.1016/j.icarus.2019.113443)
- Thuillet, F., Michel, P., Maurel, C., et al. 2018, *Astronomy & Astrophysics*, 615, A41, doi: [10.1051/0004-6361/201832779](https://doi.org/10.1051/0004-6361/201832779)
- Watanabe, S., Hirabayashi, M., Hirata, N., et al. 2019, *Science*, 364, 268, doi: [10.1126/science.aav8032](https://doi.org/10.1126/science.aav8032)
- Wendell, D. M., Luginbuhl, K., Guerrero, J., & Hosoi, A. E. 2012, *Experimental Mechanics*, 52, 945, doi: [10.1007/s11340-011-9569-x](https://doi.org/10.1007/s11340-011-9569-x)

Wilkinson, R. A., Behringer, R. P., Jenkins, J. T., & Louge, M. Y. 2005, AIP Conference Proceedings, 746, 1216, doi: [10.1063/1.1867248](https://doi.org/10.1063/1.1867248)

Woerner, J., Foing, B., & Moon Village International Support Group. 2016, in Annual Meeting of the Lunar Exploration Analysis Group, Vol. 1960, 5084

Zacny, K., Bierhaus, E. B., T. Britt, D., et al. 2018, in Primitive Meteorites and Asteroids, ed. N. Abreu (Elsevier), 439–476, doi: [10.1016/B978-0-12-813325-5.00008-2](https://doi.org/10.1016/B978-0-12-813325-5.00008-2)